Supporting Information Appendix

Structure and function of yeast Atg20, a sorting nexin that facilitates autophagy induction

Hana Popelka[1], Alejandro Damasio[2], Jenny E. Hinshaw[3], Daniel J. Klionsky[1,4] and Michael J. Ragusa[2]

[1]Life Sciences Institute, University of Michigan, Ann Arbor, MI 48109, USA

[2]Deparment of Chemistry, Dartmouth College, Hanover, NH 03755, USA

[3]Laboratory of Cell and Molecular Biology, National Institutes of Health, Bethesda, MD 20892, USA

[4]Department of Molecular, Cellular, and Developmental Biology, University of Michigan, Ann Arbor, MI 48109, USA

Fig. S1. Atg20 is essential for the efficient initiation of nonselective autophagy. Wild-type and *atg20*Δ cells were monitored using the (*A*) Pho8Δ60 assay and (*B*) GFP-Atg8 processing assay (strains ZFY202 and YAB87). (*C*) The *vac8*Δ and *atg20*Δ *vac8*Δ strains were examined for prApe1 maturation (strains HPY081 and HPY082) as described in the legend for Figure 1C.

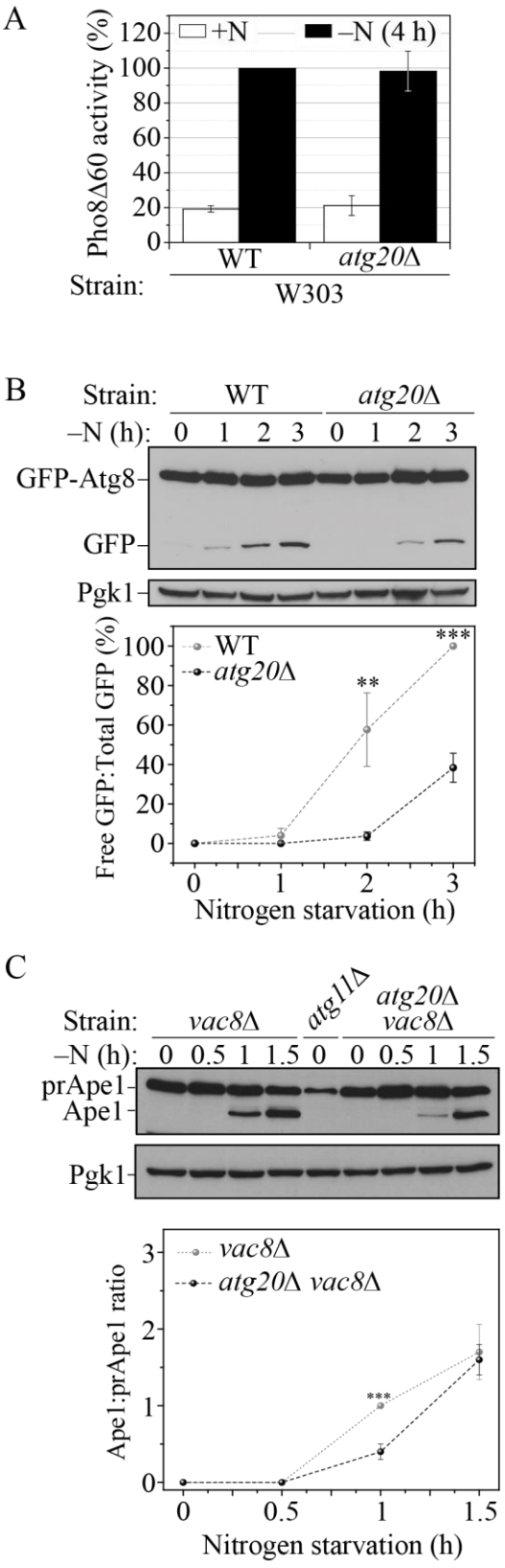

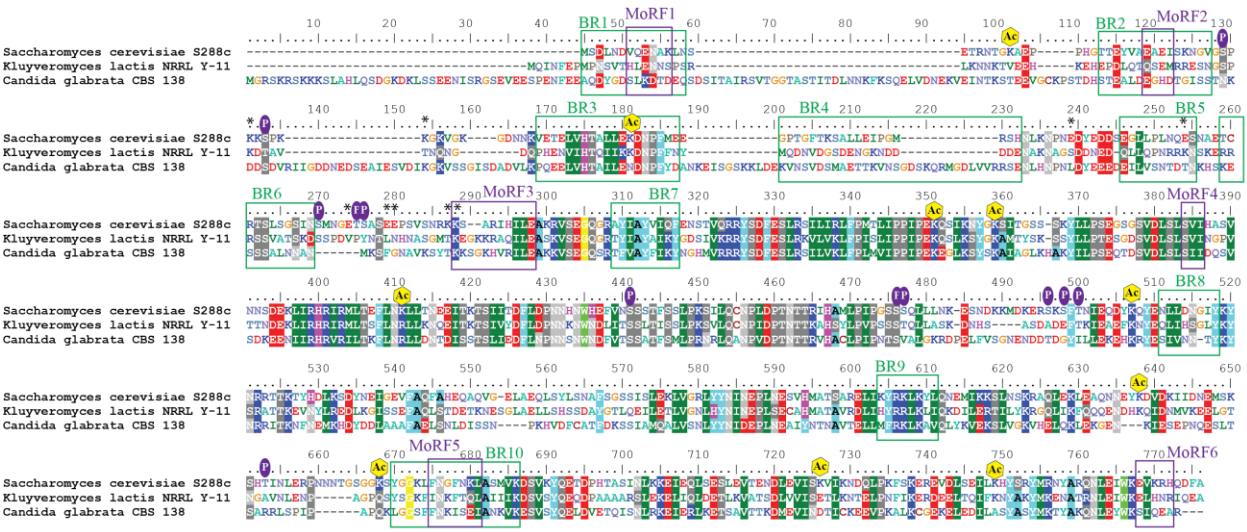

Fig. S2. Multiple sequence alignment of Atg20 proteins from three fungi that are often used in autophagy studies. Phosphorylation (P) and acetylation (Ac) sites for the *S. cerevisiae* sequence are marked. Predicted BR and MoRF regions from the *S. cerevisiae* sequence are boxed in green and purple respectively. Black asterisks show the amino acid residues mutated in the Atg20[Aroma] mutant.

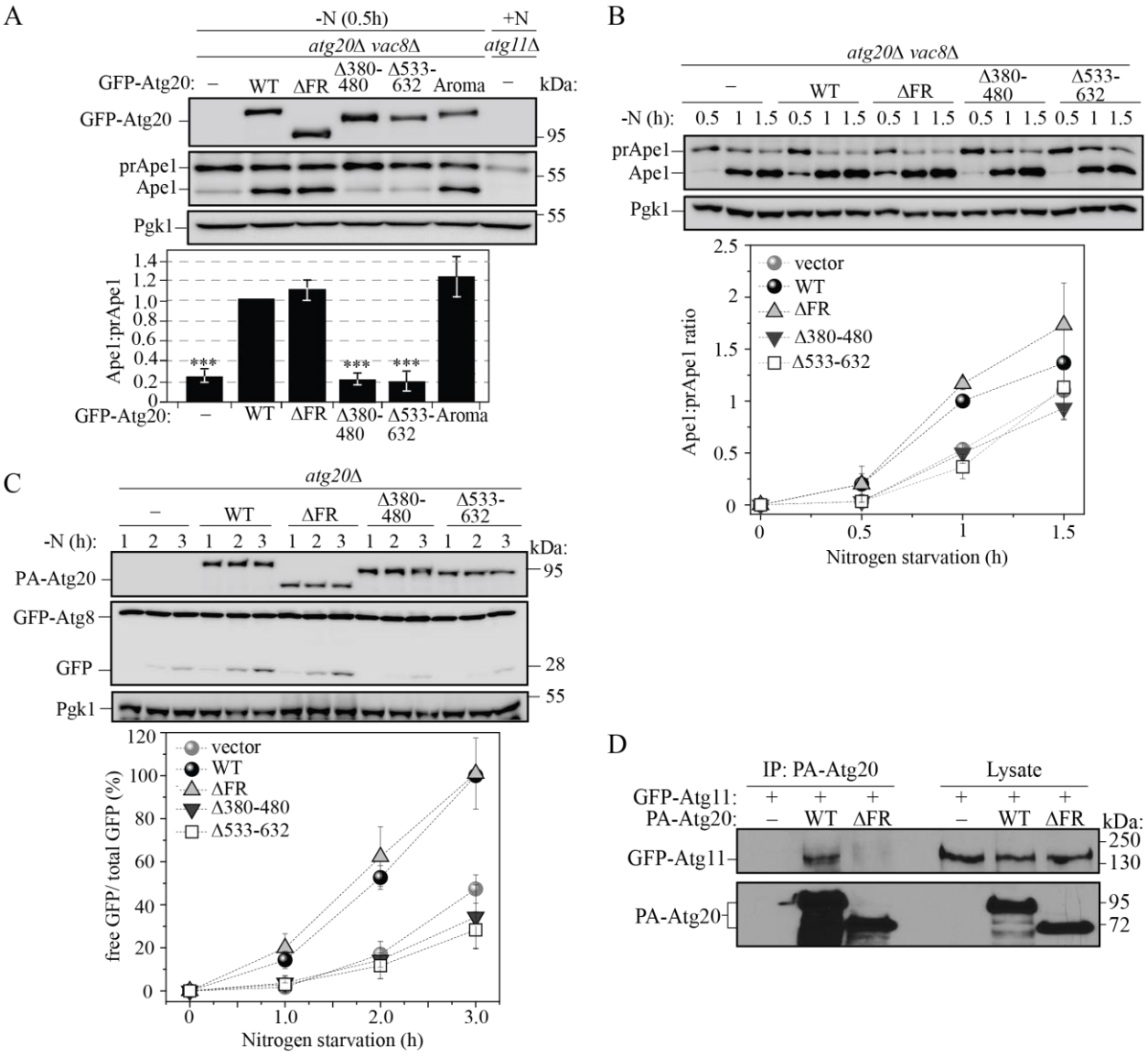

Fig. S3. Functionality and binding properties of Atg20 mutants. (*A*) The prApe1 maturation in *atg20*Δ *vac8*Δ (HPY079) cells transformed with the plasmids pCuGFP(426), pCuGFP-Atg20(426), pCuGFP-Atg20[ΔFR](426), pCuGFP-Atg20[Δ380-480](426), pCuGFP-Atg20[Δ533-632](426) or pCuGFP-Atg20[Aroma](426), cultured in rich selective medium and then nitrogen starved for 0.5 h. Statistical significance was tested by unpaired two-tailed Student's t-test. The p values less than 0.005 were considered to be significant (***). (*B*) Kinetics of prApe1 maturation after the shift to nitrogen starvation medium for the indicated times. Deletion mutants of Atg20 were compared to empty vector and wild-type Atg20. (*C*) Kinetics of GFP-Atg8 processing during nitrogen starvation for the indicated times. The *atg20*Δ (D3Y009)

cells were transformed with the plasmid pCuGFP-Atg8 (426) and the plasmid pCuPA(424), pCuPA-Atg20(424), pCuPA-Atg20[ΔFR](424), pCuPA-Atg20[Δ380-480](424), or pCuPA-Atg20[Δ533-632](424). Error bars represent standard deviation from 3 independent experiments. (*D*) Deletion of Atg20 FR weakens the interaction between Atg20 and Atg11. The plasmids pCuPA(424) or pCuPA-Atg20(424) were transformed into *atg20*Δ (D3Y009) cells and co-expressed with a plasmid encoding GFP-Atg11 (pCuGFP-Atg11; 416) under the *CUP1* promotor. The large GFP tag at Atg11 completely abolished interaction with the deletion mutant of Atg20. Cells were cultured in SMD media and cell lysates were prepared and incubated with IgG-Sepharose for affinity purification. The proteins were separated by SDS-PAGE and detected with monoclonal antibody that recognizes HA or PA or GFP.

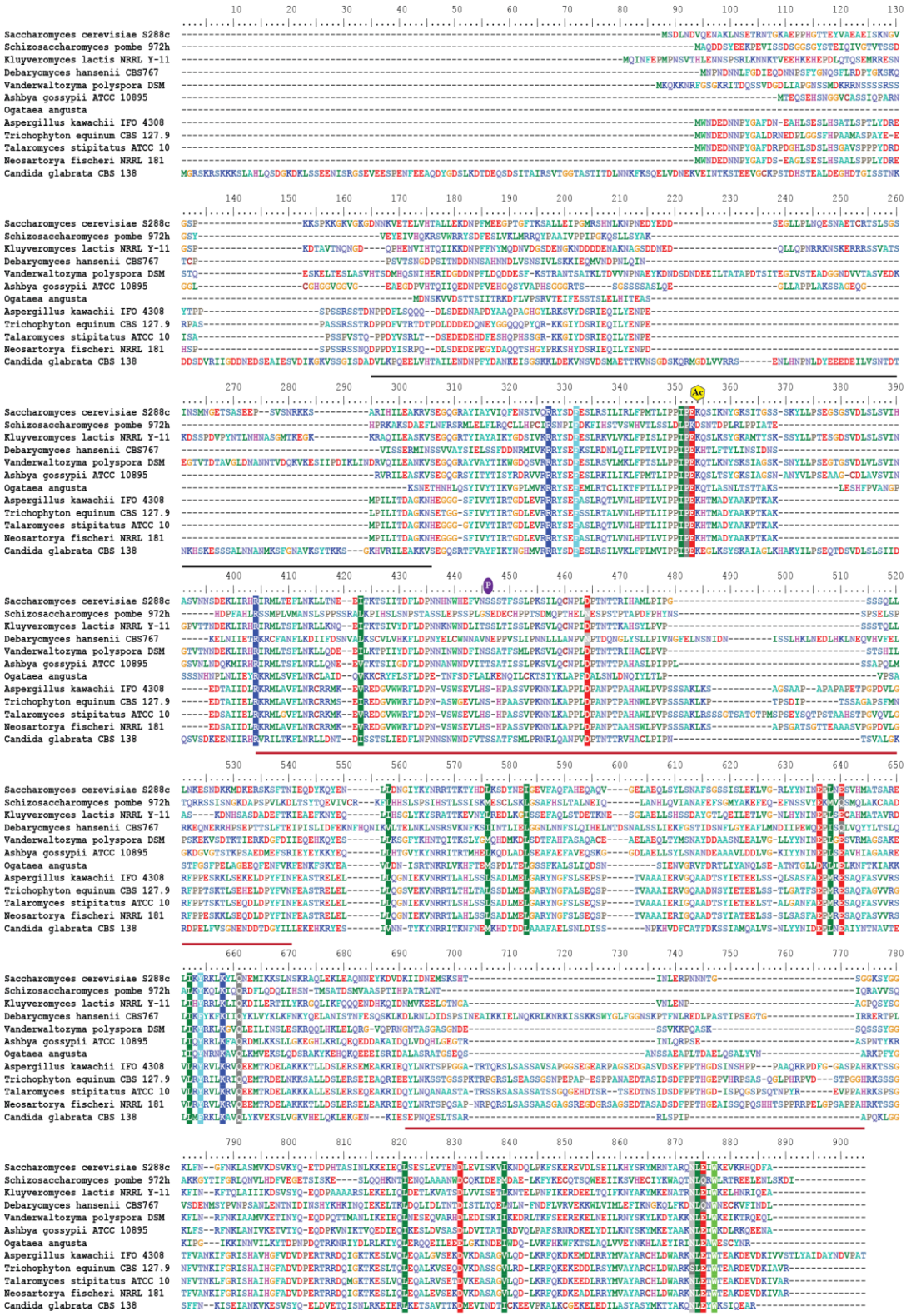

Fig. S4. Multiple sequence alignment of Atg20 proteins from various fungi. The alignment was created in the BioEdit Sequence Alignment Editor (1). The most conserved acetylated lysine

(K218) and phosphorylated serine (S307) in *S cerevisiae* are marked. The black and red lines above the sequences denote the span of the PX and BAR domain in *S. cerevisiae*, respectively.

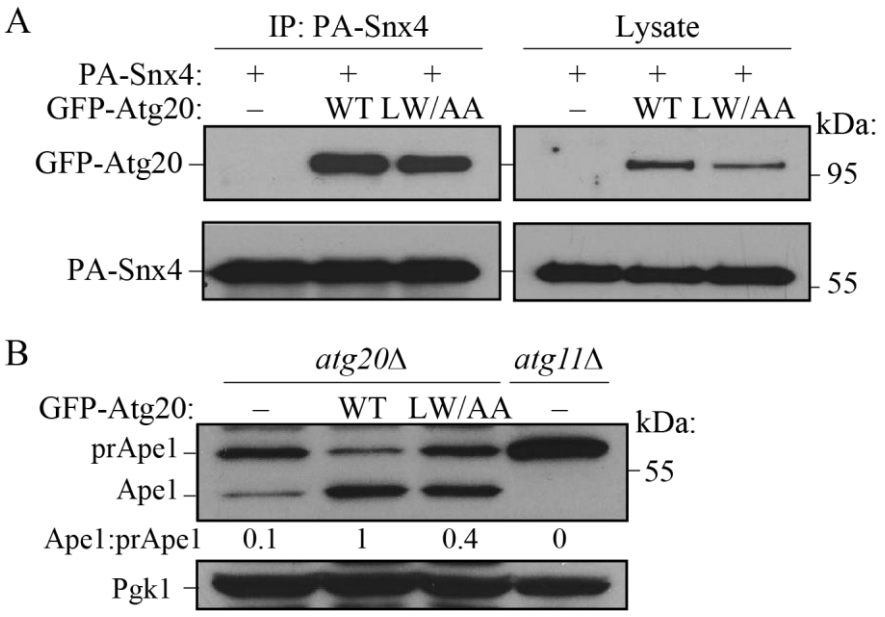

Fig. S5. Probing the conserved motif $_{626}$NLExW in Atg20. (*A*) The plasmids pCuGFP(426), pCuGFP-Atg20(426) or pCuGFP-Atg20[L627A/W630A](426) were transformed into MKO (YCY123) cells and co-expressed under the *CUP1* promotor with a plasmid encoding PA-Snx4 (pCuPA-Snx4; 424). Cells were cultured in SMD, and cell lysates were prepared and incubated with IgG-Sepharose for affinity purification. The proteins were separated by SDS-PAGE and detected with monoclonal antibody that recognizes GFP or PA. (*B*) PrApe1 processing assay. The *atg20*Δ (D3Y009) strain was transformed with the plasmid pCuGFP(426), pCuGFP-Atg20(426) or pCuGFP-Atg20[L627A/W630A](426). The *atg11*Δ strain (SEY6210) was used as a negative control. Cells were cultured in rich selective medium and cell lysates were TCA precipitated. Proteins were detected by Ape1 and Pgk1 antibody after separation on SDS-PAGE.

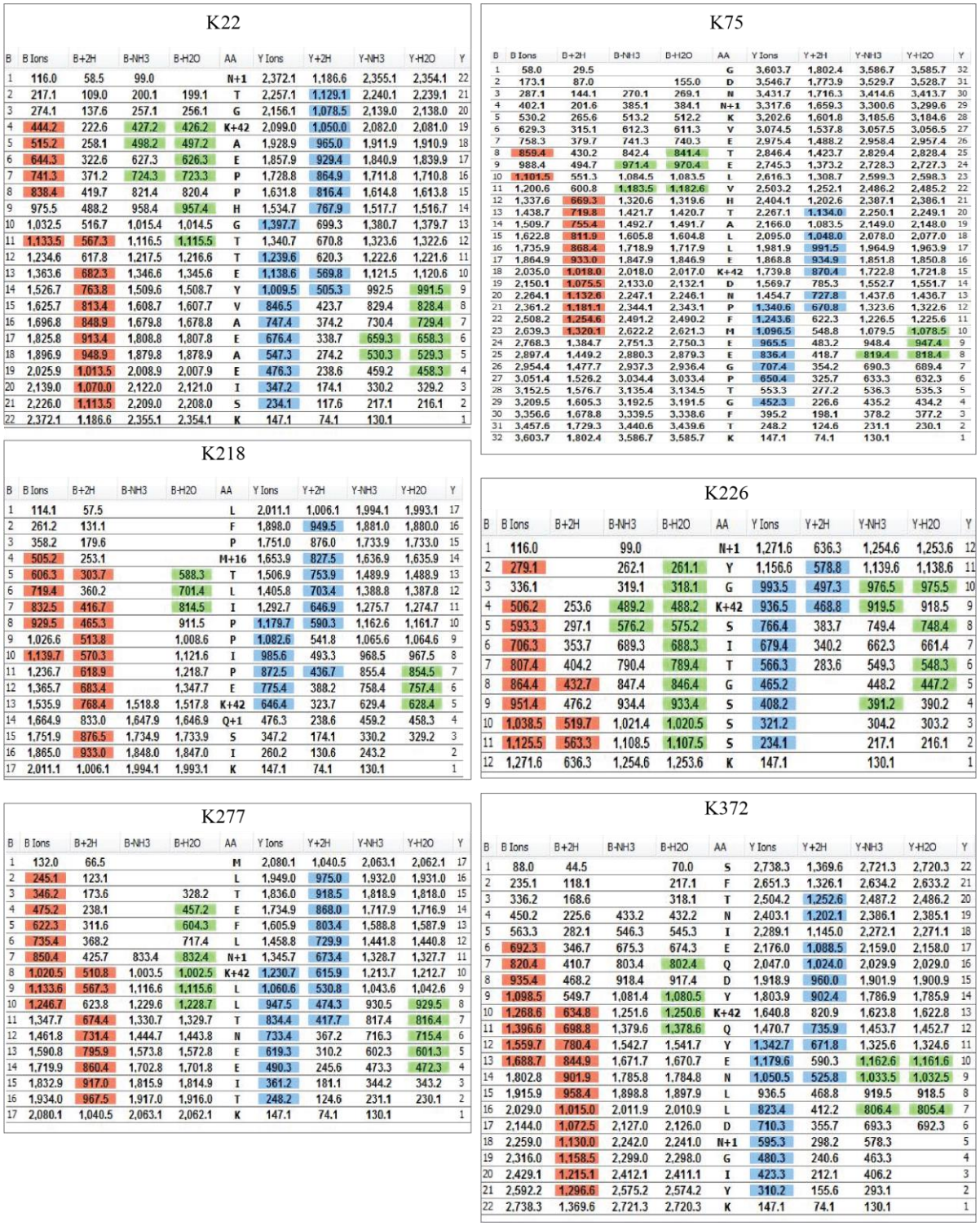

K22

B	B Ions	B+2H	B-NH3	B-H2O	AA	Y Ions	Y+2H	Y-NH3	Y-H2O	Y
1	116.0	58.5	99.0		N+1	2,372.1	1,186.6	2,355.1	2,354.1	22
2	217.1	109.0	200.1	199.1	T	2,257.1	1,129.1	2,240.1	2,239.1	21
3	274.1	137.6	257.1	256.1	G	2,156.1	1,078.5	2,139.0	2,138.0	20
4	444.2	222.6	427.2	426.2	K+42	2,099.0	1,050.0	2,082.0	2,081.0	19
5	515.2	258.1	498.2	497.2	A	1,928.9	965.0	1,911.9	1,910.9	18
6	644.3	322.6	627.3	626.3	E	1,857.9	929.4	1,840.9	1,839.9	17
7	741.3	371.2	724.3	723.3	P	1,728.8	864.9	1,711.8	1,710.8	16
8	838.4	419.7	821.4	820.4	P	1,631.8	816.4	1,614.8	1,613.8	15
9	975.5	488.2	958.4	957.4	H	1,534.7	767.9	1,517.7	1,516.7	14
10	1,032.5	516.7	1,015.4	1,014.5	G	1,397.7	699.3	1,380.7	1,379.7	13
11	1,133.5	567.3	1,116.5	1,115.5	T	1,340.7	670.8	1,323.6	1,322.6	12
12	1,234.6	617.8	1,217.5	1,216.6	T	1,239.6	620.3	1,222.6	1,221.6	11
13	1,363.6	682.3	1,346.6	1,345.6	E	1,138.6	569.8	1,121.5	1,120.6	10
14	1,526.7	763.8	1,509.6	1,508.7	Y	1,009.5	505.3	992.5	991.5	9
15	1,625.7	813.4	1,608.7	1,607.7	V	846.5	423.7	829.4	828.4	8
16	1,696.8	848.9	1,679.8	1,678.8	A	747.4	374.2	730.4	729.4	7
17	1,825.8	913.4	1,808.8	1,807.8	E	676.4	338.7	659.3	658.3	6
18	1,896.9	948.9	1,879.8	1,878.9	A	547.3	274.2	530.3	529.3	5
19	2,025.9	1,013.5	2,008.9	2,007.9	E	476.3	238.6	459.2	458.3	4
20	2,139.0	1,070.0	2,122.0	2,121.0	I	347.2	174.1	330.2	329.2	3
21	2,226.0	1,113.5	2,209.0	2,208.0	S	234.1	117.6	217.1	216.1	2
22	2,372.1	1,186.6	2,355.1	2,354.1	K	147.1	74.1	130.1		1

K75

B	B Ions	B+2H	B-NH3	B-H2O	AA	Y Ions	Y+2H	Y-NH3	Y-H2O	Y
1	58.0	29.5			G	3,603.7	1,802.4	3,586.7	3,585.7	32
2	173.1	87.0		155.0	D	3,546.7	1,773.9	3,529.7	3,528.7	31
3	287.1	144.1	270.1	269.1	N	3,431.7	1,716.3	3,414.6	3,413.7	30
4	402.1	201.6	385.1	384.1	N+1	3,317.6	1,659.3	3,300.6	3,299.6	29
5	530.2	265.6	513.2	512.2	K	3,202.6	1,601.8	3,185.6	3,184.6	28
6	629.3	315.1	612.3	611.3	V	3,074.5	1,537.8	3,057.5	3,056.5	27
7	758.3	379.7	741.3	740.3	E	2,975.4	1,488.2	2,958.4	2,957.4	26
8	859.4	430.2	842.4	841.4	T	2,846.4	1,423.7	2,829.4	2,828.4	25
9	988.4	494.7	971.4	970.4	E	2,745.3	1,373.2	2,728.3	2,727.3	24
10	1,101.5	551.3	1,084.5	1,083.5	L	2,616.3	1,308.7	2,599.3	2,598.3	23
11	1,200.6	600.8	1,183.5	1,182.6	V	2,503.2	1,252.1	2,486.2	2,485.2	22
12	1,337.6	669.3	1,320.6	1,319.6	H	2,404.1	1,202.6	2,387.1	2,386.1	21
13	1,438.7	719.8	1,421.7	1,420.7	T	2,267.1	1,134.0	2,250.1	2,249.1	20
14	1,509.7	755.4	1,492.7	1,491.7	A	2,166.0	1,083.5	2,149.0	2,148.0	19
15	1,622.8	811.9	1,605.8	1,604.8	L	2,095.0	1,048.0	2,078.0	2,077.0	18
16	1,735.9	868.4	1,718.9	1,717.9	L	1,981.9	991.5	1,964.9	1,963.9	17
17	1,864.9	933.0	1,847.9	1,846.9	E	1,868.8	934.9	1,851.8	1,850.8	16
18	2,035.0	1,018.0	2,018.0	2,017.0	K+42	1,739.8	870.4	1,722.8	1,721.8	15
19	2,150.1	1,075.5	2,133.0	2,132.1	D	1,569.7	785.3	1,552.7	1,551.7	14
20	2,264.1	1,132.6	2,247.1	2,246.1	N	1,454.7	727.8	1,437.6	1,436.7	13
21	2,361.2	1,181.1	2,344.1	2,343.1	P	1,340.6	670.8	1,323.6	1,322.6	12
22	2,508.2	1,254.6	2,491.2	2,490.2	F	1,243.6	622.3	1,226.5	1,225.6	11
23	2,639.3	1,320.1	2,622.2	2,621.3	M	1,096.5	548.8	1,079.5	1,078.5	10
24	2,768.3	1,384.7	2,751.3	2,750.3	E	965.5	483.2	948.4	947.4	9
25	2,897.4	1,449.2	2,880.3	2,879.3	E	836.4	418.7	819.4	818.4	8
26	2,954.4	1,477.7	2,937.3	2,936.4	G	707.4	354.2	690.3	689.4	7
27	3,051.4	1,526.2	3,034.4	3,033.4	P	650.4	325.7	633.3	632.3	6
28	3,152.5	1,576.7	3,135.4	3,134.5	T	553.3	277.2	536.3	535.3	5
29	3,209.5	1,605.3	3,192.5	3,191.5	G	452.3	226.6	435.2	434.2	4
30	3,356.6	1,678.8	3,339.5	3,338.6	F	395.2	198.1	378.2	377.2	3
31	3,457.6	1,729.3	3,440.6	3,439.6	T	248.2	124.6	231.1	230.1	2
32	3,603.7	1,802.4	3,586.7	3,585.7	K	147.1	74.1	130.1		1

K218

B	B Ions	B+2H	B-NH3	B-H2O	AA	Y Ions	Y+2H	Y-NH3	Y-H2O	Y
1	114.1	57.5			L	2,011.1	1,006.1	1,994.1	1,993.1	17
2	261.2	131.1			F	1,898.0	949.5	1,881.0	1,880.0	16
3	358.2	179.6			P	1,751.0	876.0	1,733.9	1,733.0	15
4	505.2	253.1			M+16	1,653.9	827.5	1,636.9	1,635.9	14
5	606.3	303.7		588.3	T	1,506.9	753.9	1,489.9	1,488.9	13
6	719.4	360.2		701.4	L	1,405.8	703.4	1,388.8	1,387.8	12
7	832.5	416.7		814.5	I	1,292.7	646.9	1,275.7	1,274.7	11
8	929.5	465.3		911.5	P	1,179.7	590.3	1,162.6	1,161.7	10
9	1,026.6	513.8		1,008.6	P	1,082.6	541.8	1,065.6	1,064.6	9
10	1,139.7	570.3		1,121.6	I	985.6	493.3	968.5	967.5	8
11	1,236.7	618.9		1,218.7	P	872.5	436.7	855.4	854.5	7
12	1,365.7	683.4		1,347.7	E	775.4	388.2	758.4	757.4	6
13	1,535.9	768.4	1,518.8	1,517.8	K+42	646.4	323.7	629.4	628.4	5
14	1,664.9	833.0	1,647.9	1,646.9	Q+1	476.3	238.6	459.2	458.3	4
15	1,751.9	876.5	1,734.9	1,733.9	S	347.2	174.1	330.2	329.2	3
16	1,865.0	933.0	1,848.0	1,847.0	I	260.2	130.6	243.2		2
17	2,011.1	1,006.1	1,994.1	1,993.1	K	147.1	74.1	130.1		1

K226

B	B Ions	B+2H	B-NH3	B-H2O	AA	Y Ions	Y+2H	Y-NH3	Y-H2O	Y
1	116.0		99.0		N+1	1,271.6	636.3	1,254.6	1,253.6	12
2	279.1		262.1	261.1	Y	1,156.6	578.8	1,139.6	1,138.6	11
3	336.1		319.1	318.1	G	993.5	497.3	976.5	975.5	10
4	506.2	253.6	489.2	488.2	K+42	936.5	468.8	919.5	918.5	9
5	593.3	297.1	576.2	575.2	S	766.4	383.7	749.4	748.4	8
6	706.3	353.7	689.3	688.3	I	679.4	340.2	662.3	661.4	7
7	807.4	404.2	790.4	789.4	T	566.3	283.6	549.3	548.3	6
8	864.4	432.7	847.4	846.4	G	465.2		448.2	447.2	5
9	951.4	476.2	934.4	933.4	S	408.2		391.2	390.2	4
10	1,038.5	519.7	1,021.4	1,020.5	S	321.2		304.2	303.2	3
11	1,125.5	563.3	1,108.5	1,107.5	S	234.1		217.1	216.1	2
12	1,271.6	636.3	1,254.6	1,253.6	K	147.1		130.1		1

K277

B	B Ions	B+2H	B-NH3	B-H2O	AA	Y Ions	Y+2H	Y-NH3	Y-H2O	Y
1	132.0	66.5			M	2,080.1	1,040.5	2,063.1	2,062.1	17
2	245.1	123.1			L	1,949.0	975.0	1,932.0	1,931.0	16
3	346.2	173.6		328.2	T	1,836.0	918.5	1,818.9	1,818.0	15
4	475.2	238.1		457.2	E	1,734.9	868.0	1,717.9	1,716.9	14
5	622.3	311.6		604.3	F	1,605.9	803.4	1,588.8	1,587.9	13
6	735.4	368.2		717.4	L	1,458.8	729.9	1,441.8	1,440.8	12
7	850.4	425.7	833.4	832.4	N+1	1,345.7	673.4	1,328.7	1,327.7	11
8	1,020.5	510.8	1,003.5	1,002.5	K+42	1,230.7	615.9	1,213.7	1,212.7	10
9	1,133.6	567.3	1,116.6	1,115.6	L	1,060.6	530.8	1,043.6	1,042.6	9
10	1,246.7	623.8	1,229.6	1,228.7	L	947.5	474.3	930.5	929.5	8
11	1,347.7	674.4	1,330.7	1,329.7	T	834.4	417.7	817.4	816.4	7
12	1,461.8	731.4	1,444.7	1,443.8	N	733.4	367.2	716.3	715.4	6
13	1,590.8	795.9	1,573.8	1,572.8	E	619.3	310.2	602.3	601.3	5
14	1,719.9	860.4	1,702.8	1,701.8	E	490.3	245.6	473.3	472.3	4
15	1,832.9	917.0	1,815.9	1,814.9	I	361.2	181.1	344.2	343.2	3
16	1,934.0	967.5	1,917.0	1,916.0	T	248.2	124.6	231.1	230.1	2
17	2,080.1	1,040.5	2,063.1	2,062.1	K	147.1	74.1	130.1		1

K372

B	B Ions	B+2H	B-NH3	B-H2O	AA	Y Ions	Y+2H	Y-NH3	Y-H2O	Y
1	88.0	44.5		70.0	S	2,738.3	1,369.6	2,721.3	2,720.3	22
2	235.1	118.1		217.1	F	2,651.3	1,326.1	2,634.2	2,633.2	21
3	336.2	168.6		318.1	T	2,504.2	1,252.6	2,487.2	2,486.2	20
4	450.2	225.6	433.2	432.2	N	2,403.1	1,202.1	2,386.1	2,385.1	19
5	563.3	282.1	546.3	545.3	I	2,289.1	1,145.0	2,272.1	2,271.1	18
6	692.3	346.7	675.3	674.3	E	2,176.0	1,088.5	2,159.0	2,158.0	17
7	820.4	410.7	803.4	802.4	Q	2,047.0	1,024.0	2,029.9	2,029.0	16
8	935.4	468.2	918.4	917.4	D	1,918.9	960.0	1,901.9	1,900.9	15
9	1,098.5	549.7	1,081.4	1,080.5	Y	1,803.9	902.4	1,786.9	1,785.9	14
10	1,268.6	634.8	1,251.6	1,250.6	K+42	1,640.8	820.9	1,623.8	1,622.8	13
11	1,396.6	698.8	1,379.6	1,378.6	Q	1,470.7	735.9	1,453.7	1,452.7	12
12	1,559.7	780.4	1,542.7	1,541.7	Y	1,342.7	671.8	1,325.6	1,324.6	11
13	1,688.7	844.9	1,671.7	1,670.7	E	1,179.6	590.3	1,162.6	1,161.6	10
14	1,802.8	901.9	1,785.8	1,784.8	N	1,050.5	525.8	1,033.5	1,032.5	9
15	1,915.9	958.4	1,898.8	1,897.9	L	936.5	468.8	919.5	918.5	8
16	2,029.0	1,015.0	2,011.9	2,010.9	L	823.4	412.2	806.4	805.4	7
17	2,144.0	1,072.5	2,127.0	2,126.0	D	710.3	355.7	693.3	692.3	6
18	2,259.0	1,130.0	2,242.0	2,241.0	N+1	595.3	298.2	578.3		5
19	2,316.0	1,158.5	2,299.0	2,298.0	G	480.3	240.6	463.3		4
20	2,429.1	1,215.1	2,412.1	2,411.1	I	423.3	212.1	406.2		3
21	2,592.2	1,296.6	2,575.2	2,574.2	Y	310.2	155.6	293.1		2
22	2,738.3	1,369.6	2,721.3	2,720.3	K	147.1	74.1	130.1		1

Fig. S6. Fragmentation tables as they appear in the Scaffold program for acetylated lysines (K22, K75, K218, K226, K277, and K372) in Atg20. The presence of acetylated lysine (K+42) is confirmed by *b* and/or *y* ions that are highlighted in red and blue color.

K502

B	B Ions	B+2H	B-NH3	B-H2O	AA	Y Ions	Y+2H	Y-NH3	Y-H2O	Y
1	114.1	57.5			L	2,555.2	1,278.1	2,538.2	2,537.2	21
2	243.1	122.1		225.1	E	2,442.1	1,221.6	2,425.1	2,424.1	20
3	314.2	157.6		296.2	A	2,313.1	1,157.0	2,296.0	2,295.0	19
4	442.2	221.6	425.2	424.2	Q	2,242.0	1,121.5	2,225.0	2,224.0	18
5	557.3	279.1	540.2	539.2	N+1	2,114.0	1,057.5	2,096.9	2,095.9	17
6	671.3	336.2	654.3	653.3	N	1,998.9	1,000.0	1,981.9	1,980.9	16
7	800.3	400.7	783.3	782.3	E	1,884.9	942.9	1,867.9	1,866.9	15
8	963.4	482.2	946.4	945.4	Y	1,755.8	878.4	1,738.8	1,737.8	14
9	1,133.5	567.3	1,116.5	1,115.5	K+42	1,592.8	796.9	1,575.8	1,574.8	13
10	1,248.5	624.8	1,231.5	1,230.5	D	1,422.7	711.8	1,405.7	1,404.7	12
11	1,347.6	674.3	1,330.6	1,329.6	V	1,307.7	654.3	1,290.6	1,289.6	11
12	1,462.6	731.8	1,445.6	1,444.6	D	1,208.6	604.8	1,191.6	1,190.6	10
13	1,590.7	795.9	1,573.7	1,572.7	K	1,093.6	547.3	1,076.5	1,075.5	9
14	1,703.8	852.4	1,686.8	1,685.8	I	965.5	483.2	948.4	947.5	8
15	1,816.9	909.0	1,799.9	1,798.9	I	852.4	426.7	835.4	834.4	7
16	1,931.9	966.5	1,914.9	1,913.9	D	739.3	370.1	722.3	721.3	6
17	2,046.0	1,023.5	2,028.9	2,028.0	N	624.3	312.6	607.2	606.3	5
18	2,175.0	1,088.0	2,158.0	2,157.0	E	510.2	255.6	493.2	492.2	4
19	2,322.0	1,161.5	2,305.0	2,304.0	M+16	381.2	191.1	364.2	363.2	3
20	2,409.1	1,205.0	2,392.0	2,391.1	S	234.1	117.6	217.1	216.1	2
21	2,555.2	1,278.1	2,538.2	2,537.2	K	147.1	74.1	130.1		1

K532

B	B Ions	B+2H	B-NH3	B-H2O	AA	Y Ions	Y+2H	Y-NH3	Y-H2O	Y
1	88.0	44.5		70.0	S	2,430.2	1,215.6	2,413.1	2,412.2	23
2	225.1	113.1		207.1	H	2,343.1	1,172.1	2,326.1	2,325.1	22
3	326.1	163.6		308.1	T	2,206.1	1,103.5	2,189.1	2,188.1	21
4	439.2	220.1		421.2	I	2,105.0	1,053.0	2,088.0	2,087.0	20
5	553.3	277.1	536.2	535.3	N	1,992.0	996.5	1,974.9	1,973.9	19
6	666.4	333.7	649.3	648.3	L	1,877.9	939.5	1,860.9	1,859.9	18
7	795.4	398.2	778.4	777.4	E	1,764.8	882.9	1,747.8	1,746.8	17
8	951.5	476.3	934.5	933.5	R	1,635.8	818.4	1,618.8	1,617.8	16
9	1,048.6	524.8	1,031.5	1,030.5	P	1,479.7	740.3	1,462.7	1,461.7	15
10	1,162.6	581.8	1,145.6	1,144.6	N	1,382.6	691.8	1,365.6	1,364.6	14
11	1,276.6	638.8	1,259.6	1,258.6	N	1,268.6	634.8	1,251.6	1,250.6	13
12	1,390.7	695.8	1,373.7	1,372.7	N	1,154.5	577.8	1,137.5	1,136.5	12
13	1,491.7	746.4	1,474.7	1,473.7	T	1,040.5	520.8	1,023.5	1,022.5	11
14	1,548.8	774.9	1,531.7	1,530.7	G	939.5	470.2	922.4	921.4	10
15	1,635.8	818.4	1,618.8	1,617.8	S	882.4	441.7	865.4	864.4	9
16	1,692.8	846.9	1,675.8	1,674.8	G	795.4	398.2	778.4	777.4	8
17	1,749.8	875.4	1,732.8	1,731.8	G	738.4	369.7	721.4	720.4	7
18	1,919.9	960.5	1,902.9	1,901.9	K+42	681.4	341.2	664.3	663.3	6
19	2,007.0	1,004.0	1,989.9	1,989.0	S	511.3	256.1	494.2	493.2	5
20	2,170.0	1,085.5	2,153.0	2,152.0	Y	424.2	212.6	407.2		4
21	2,227.0	1,114.0	2,210.0	2,209.0	G	261.2	131.1	244.1		3
22	2,284.1	1,142.5	2,267.0	2,266.1	G	204.1	102.6	187.1		2
23	2,430.2	1,215.6	2,413.1	2,412.2	K	147.1	74.1	130.1		1

K590

B	B Ions	B+2H	B-NH3	B-H2O	AA	Y Ions	Y+2H	Y-NH3	Y-H2O	Y
1	130.0	65.5		112.0	E	2,787.4	1,394.2	2,770.4	2,769.4	24
2	243.1	122.1		225.1	I	2,658.4	1,329.7	2,641.4	2,640.4	23
3	372.2	186.6		354.2	E	2,545.3	1,273.2	2,528.3	2,527.3	22
4	500.2	250.6	483.2	482.2	Q	2,416.3	1,208.6	2,399.2	2,398.3	21
5	613.3	307.2	596.3	595.3	L	2,288.2	1,144.6	2,271.2	2,270.2	20
6	700.4	350.7	683.3	682.3	S	2,175.1	1,088.1	2,158.1	2,157.1	19
7	829.4	415.2	812.4	811.4	E	2,088.1	1,044.6	2,071.1	2,070.1	18
8	916.4	458.7	899.4	898.4	S	1,959.1	980.0	1,942.0	1,941.0	17
9	1,029.5	515.3	1,012.5	1,011.5	L	1,872.0	936.5	1,855.0	1,854.0	16
10	1,158.6	579.8	1,141.5	1,140.5	E	1,758.9	880.0	1,741.9	1,740.9	15
11	1,257.6	629.3	1,240.6	1,239.6	V	1,629.9	815.5	1,612.9	1,611.9	14
12	1,358.7	679.8	1,341.6	1,340.7	T	1,530.8	765.9	1,513.8	1,512.8	13
13	1,487.7	744.4	1,470.7	1,469.7	E	1,429.8	715.4	1,412.8	1,411.8	12
14	1,602.7	801.9	1,585.7	1,584.7	N+1	1,300.7	650.9	1,283.7	1,282.7	11
15	1,717.8	859.4	1,700.7	1,699.8	D	1,185.7	593.4	1,168.7	1,167.7	10
16	1,830.8	915.9	1,813.8	1,812.8	L	1,070.7	535.8	1,053.7	1,052.7	9
17	1,959.9	980.4	1,942.9	1,941.9	E	957.6	479.3	940.6	939.6	8
18	2,059.0	1,030.0	2,041.9	2,040.9	V	828.6	414.8	811.5	810.5	7
19	2,172.0	1,086.5	2,155.0	2,154.0	I	729.5	365.2	712.5	711.5	6
20	2,259.1	1,130.0	2,242.0	2,241.1	S	616.4	308.7	599.4	598.4	5
21	2,429.2	1,215.1	2,412.2	2,411.2	K+42	529.4	265.2	512.3		4
22	2,528.2	1,264.6	2,511.2	2,510.2	V	359.3	180.1	342.2		3
23	2,641.3	1,321.2	2,624.3	2,623.3	I	260.2	130.6	243.2		2
24	2,787.4	1,394.2	2,770.4	2,769.4	K	147.1	74.1	130.1		1

K613

B	B Ions	B+2H	B-NH3	B-H2O	AA	Y Ions	Y+2H	Y-NH3	Y-H2O	Y
1	130.0	65.5		112.0	E	1,916.0	958.5	1,899.0	1,898.0	15
2	286.2	143.6	269.1	268.1	R	1,786.9	894.0	1,769.9	1,768.9	14
3	415.2	208.1	398.2	397.2	E	1,630.8	815.9	1,613.8	1,612.8	13
4	514.3	257.6	497.2	496.3	V	1,501.8	751.4	1,484.8	1,483.8	12
5	629.3	315.1	612.3	611.3	D	1,402.7	701.9	1,385.7	1,384.7	11
6	742.4	371.7	725.3	724.4	L	1,287.7	644.4	1,270.7	1,269.7	10
7	829.4	415.2	812.4	811.4	S	1,174.6	587.8	1,157.6	1,156.6	9
8	958.4	479.7	941.4	940.4	E	1,087.6	544.3	1,070.6	1,069.6	8
9	1,071.5	536.3	1,054.5	1,053.5	I	958.5	479.8	941.5	940.5	7
10	1,184.6	592.8	1,167.6	1,166.6	L	845.5	423.2	828.4	827.5	6
11	1,354.7	677.9	1,337.7	1,336.7	K+42	732.4	366.7	715.4	714.4	5
12	1,491.8	746.4	1,474.8	1,473.8	H	562.3	281.6	545.2	544.3	4
13	1,654.8	827.9	1,637.8	1,636.8	Y	425.2	213.1	408.2	407.2	3
14	1,741.9	871.4	1,724.8	1,723.9	S	262.2	131.6	245.1	244.1	2
15	1,916.0	958.5	1,899.0	1,898.0	R	175.1	88.1	158.1		1

Fig. S7. Fragmentation tables as they appear in the Scaffold program for acetylated lysines (K502, K532, K590, and K613) in Atg20. The presence of acetylated lysine (K+42) is confirmed by *b* and/or *y* ions that are highlighted in red and blue color.

S45 , S49

B	B Ions	B+2H	B-NH3	B-H2O	AA	Y Ions	Y+2H	Y-NH3	Y-H2O	Y
1	115.1		98.0		N	1,258.6	629.8	1,241.5	1,240.5	11
2	172.1		155.0		G	1,144.5	572.8	1,127.5	1,126.5	10
3	271.1		254.1		V	1,087.5	544.3	1,070.5	1,069.5	9
4	328.2		311.1		G	988.4	494.7	971.4	970.4	8
5	495.2		478.1	477.1	S+80	931.4	466.2	914.4	913.4	7
6	592.2	296.6	575.2	574.2	P	764.4	382.7	747.4	746.4	6
7	720.3	360.7	703.3	702.3	K	667.4	334.2	650.3	649.3	5
8	848.4	424.7	831.4	830.4	K	539.3	270.1	522.2	521.2	4
9	1,015.4	508.2	998.4	997.4	S+80	411.2		394.1	393.2	3
10	1,112.5	556.7	1,095.4	1,094.4	P	244.2		227.1		2
11	1,258.6	629.8	1,241.5	1,240.5	K	147.1		130.1		1

T144

B	B Ions	B+2H	B-NH3	B-H2O	AA	Y Ions	Y+2H	Y-NH3	Y-H2O	Y
1	102.1	51.5		84.0	T	2,622.1	1,311.5	2,605.1	2,604.1	25
2	189.1	95.0		171.1	S	2,521.0	1,261.0	2,504.0	2,503.0	24
3	302.2	151.6		284.2	L	2,434.0	1,217.5	2,417.0	2,416.0	23
4	389.2	195.1		371.2	S	2,320.9	1,161.0	2,303.9	2,302.9	22
5	446.2	223.6		428.2	G	2,233.9	1,117.4	2,216.9	2,215.9	21
6	533.3	267.1		515.2	S	2,176.9	1,088.9	2,159.8	2,158.9	20
7	646.3	323.7		628.3	I	2,089.8	1,045.4	2,072.8	2,071.8	19
8	760.4	380.7	743.4	742.4	N	1,976.8	988.9	1,959.7	1,958.7	18
9	847.4	424.2	830.4	829.4	S	1,862.7	931.9	1,845.7	1,844.7	17
10	978.5	489.7	961.4	960.4	M	1,775.7	888.3	1,758.7	1,757.7	16
11	1,093.5	547.2	1,076.5	1,075.5	N+1	1,644.6	822.8	1,627.6	1,626.6	15
12	1,150.5	575.8	1,133.5	1,132.5	G	1,529.6	765.3	1,512.6	1,511.6	14
13	1,279.5	640.3	1,262.5	1,261.5	E	1,472.6	736.8	1,455.6	1,454.6	13
14	1,460.6	730.8	1,443.5	1,442.6	T+80	1,343.5	672.3	1,326.5	1,325.5	12
15	1,547.6	774.3	1,530.6	1,529.6	S	1,162.5	581.8	1,145.5	1,144.5	11
16	1,618.6	809.8	1,601.6	1,600.6	A	1,075.5	538.3	1,058.5	1,057.5	10
17	1,705.7	853.3	1,688.6	1,687.7	S	1,004.5	502.7	987.4	986.5	9
18	1,834.7	917.9	1,817.7	1,816.7	E	917.4	459.2	900.4	899.4	8
19	1,963.7	982.4	1,946.7	1,945.7	E	788.4	394.7	771.4	770.4	7
20	2,060.8	1,030.9	2,043.8	2,042.8	P	659.3	330.2	642.3	641.3	6
21	2,147.8	1,074.4	2,130.8	2,129.8	S	562.3	281.7	545.3	544.3	5
22	2,246.9	1,124.0	2,229.9	2,228.9	V	475.3	238.1	458.2	457.3	4
23	2,333.9	1,167.5	2,316.9	2,315.9	S	376.2	188.6	359.2	358.2	3
24	2,448.0	1,224.5	2,430.9	2,430.0	N	289.2	145.1	272.1		2
25	2,622.1	1,311.5	2,605.1	2,604.1	R	175.1	88.1	158.1		1

S307

B	B Ions	B+2H	B-NH3	B-H2O	AA	Y Ions	Y+2H	Y-NH3	Y-H2O	Y
1	102.1	51.5		84.0	T	3,514.6	1,757.8	3,497.6	3,496.6	30
2	189.1	95.0		171.1	S	3,413.5	1,707.3	3,396.5	3,395.5	29
3	302.2	151.6		284.2	I	3,326.5	1,663.8	3,309.5	3,308.5	28
4	415.3	208.1		397.2	I	3,213.4	1,607.2	3,196.4	3,195.4	27
5	516.3	258.7		498.3	T	3,100.3	1,550.7	3,083.3	3,082.3	26
6	631.3	316.2		613.3	D	2,999.3	1,500.2	2,982.3	2,981.3	25
7	778.4	389.7		760.4	F	2,884.3	1,442.6	2,867.2	2,866.3	24
8	891.5	446.2		873.5	L	2,737.2	1,369.1	2,720.2	2,719.2	23
9	1,006.5	503.8		988.5	D	2,624.1	1,312.6	2,607.1	2,606.1	22
10	1,103.6	552.3		1,085.6	P	2,509.1	1,255.1	2,492.1	2,491.1	21
11	1,217.6	609.3	1,200.6	1,199.6	N	2,412.0	1,206.5	2,395.0	2,394.0	20
12	1,331.6	666.3	1,314.6	1,313.6	N	2,298.0	1,149.5	2,281.0	2,280.0	19
13	1,468.7	734.9	1,451.7	1,450.7	H	2,184.0	1,092.5	2,166.9	2,165.9	18
14	1,582.7	791.9	1,565.7	1,564.7	N	2,046.9	1,024.0	2,029.9	2,028.9	17
15	1,768.8	884.9	1,751.8	1,750.8	W	1,932.9	966.9	1,915.8	1,914.8	16
16	1,905.9	953.4	1,888.9	1,887.9	H	1,746.8	873.9	1,729.7	1,728.8	15
17	2,034.9	1,018.0	2,017.9	2,016.9	E	1,609.7	805.4	1,592.7	1,591.7	14
18	2,182.0	1,091.5	2,165.0	2,164.0	F	1,480.7	740.8	1,463.6	1,462.7	13
19	2,281.1	1,141.0	2,264.0	2,263.1	V	1,333.6	667.3	1,316.6	1,315.6	12
20	2,395.1	1,198.1	2,378.1	2,377.1	N	1,234.5	617.8	1,217.5	1,216.5	11
21	2,562.1	1,281.6	2,545.1	2,544.1	S+80	1,120.5	560.7	1,103.5	1,102.5	10
22	2,649.1	1,325.1	2,632.1	2,631.1	S	953.5	477.3	936.5	935.5	9
23	2,736.2	1,368.6	2,719.1	2,718.2	S	866.5	433.7	849.4	848.5	8
24	2,837.2	1,419.1	2,820.2	2,819.2	T	779.4	390.2	762.4	761.4	7
25	2,984.3	1,492.6	2,967.3	2,966.3	F	678.4	339.7	661.4	660.4	6
26	3,071.3	1,536.2	3,054.3	3,053.3	S	531.3	266.2	514.3	513.3	5
27	3,158.4	1,579.7	3,141.3	3,140.3	S	444.3	222.6	427.3	426.3	4
28	3,271.4	1,636.2	3,254.4	3,253.4	L	357.2	179.1	340.2		3
29	3,368.5	1,684.7	3,351.5	3,350.5	P	244.2	122.6	227.1		2
30	3,514.6	1,757.8	3,497.6	3,496.6	K	147.1	74.1	130.1		1

S139

B	B Ions	B+2H	B-NH3	B-H2O	AA	Y Ions	Y+2H	Y-NH3	Y-H2O	Y
1	102.1	51.5		84.0	T	2,637.1	1,319.1	2,620.1	2,619.1	25
2	189.1	95.0		171.1	S	2,536.1	1,268.5	2,519.0	2,518.0	24
3	302.2	151.6		284.2	L	2,449.0	1,225.0	2,432.0	2,431.0	23
4	389.2	195.1		371.2	S	2,335.9	1,168.5	2,318.9	2,317.9	22
5	446.2	223.6		428.2	G	2,248.9	1,125.0	2,231.9	2,230.9	21
6	533.3	267.1		515.2	S	2,191.9	1,096.4	2,174.9	2,173.9	20
7	646.3	323.7		628.3	I	2,104.8	1,052.9	2,087.8	2,086.8	19
8	760.4	380.7	743.4	742.4	N	1,991.8	996.4	1,974.7	1,973.8	18
9	927.4	464.2	910.4	909.4	S+80	1,877.7	939.4	1,860.7	1,859.7	17
10	1,074.4	537.7	1,057.4	1,056.4	M+16	1,710.7	855.9	1,693.7	1,692.7	16
11	1,188.5	594.7	1,171.4	1,170.4	N	1,563.7	782.3	1,546.7	1,545.7	15
12	1,245.5	623.2	1,228.5	1,227.5	G	1,449.6	725.3	1,432.6	1,431.6	14
13	1,374.5	687.8	1,357.5	1,356.5	E	1,392.6	696.8	1,375.6	1,374.6	13
14	1,475.6	738.3	1,458.5	1,457.6	T	1,263.6	632.3	1,246.6	1,245.6	12
15	1,562.6	781.8	1,545.6	1,544.6	S	1,162.5	581.8	1,145.5	1,144.5	11
16	1,633.6	817.3	1,616.6	1,615.6	A	1,075.5	538.3	1,058.5	1,057.5	10
17	1,720.7	860.8	1,703.6	1,702.7	S	1,004.5	502.7	987.4	986.5	9
18	1,849.7	925.4	1,832.7	1,831.7	E	917.4	459.2	900.4	899.4	8
19	1,978.8	989.9	1,961.7	1,960.7	E	788.4	394.7	771.4	770.4	7
20	2,075.8	1,038.4	2,058.8	2,057.8	P	659.3	330.2	642.3	641.3	6
21	2,162.8	1,081.9	2,145.8	2,144.8	S	562.3	281.7	545.3	544.3	5
22	2,261.9	1,131.5	2,244.9	2,243.9	V	475.3	238.1	458.2	457.3	4
23	2,348.9	1,175.0	2,331.9	2,330.9	S	376.2	188.6	359.2	358.2	3
24	2,463.0	1,232.0	2,446.0	2,445.0	N	289.2	145.1	272.1		2
25	2,637.1	1,319.1	2,620.1	2,619.1	R	175.1	88.1	158.1		1

S145

B	B Ions	B+2H	B-NH3	B-H2O	AA	Y Ions	Y+2H	Y-NH3	Y-H2O	Y
1	102.1	51.5		84.0	T	2,621.1	1,311.1	2,604.1	2,603.1	25
2	189.1	95.0		171.1	S	2,520.1	1,260.5	2,503.0	2,502.0	24
3	302.2	151.6		284.2	L	2,433.0	1,217.0	2,416.0	2,415.0	23
4	389.2	195.1		371.2	S	2,319.9	1,160.5	2,302.9	2,301.9	22
5	446.2	223.6		428.2	G	2,232.9	1,117.0	2,215.9	2,214.9	21
6	533.3	267.1		515.2	S	2,175.9	1,088.4	2,158.9	2,157.9	20
7	646.3	323.7		628.3	I	2,088.9	1,044.9	2,071.8	2,070.8	19
8	760.4	380.7	743.4	742.4	N	1,975.8	988.4	1,958.7	1,957.8	18
9	847.4	424.2	830.4	829.4	S	1,861.7	931.4	1,844.7	1,843.7	17
10	978.5	489.7	961.4	960.4	M	1,774.7	887.9	1,757.7	1,756.7	16
11	1,092.5	546.8	1,075.5	1,074.5	N	1,643.7	822.3	1,626.6	1,625.6	15
12	1,149.5	575.3	1,132.5	1,131.5	G	1,529.6	765.3	1,512.6	1,511.6	14
13	1,278.6	639.8	1,261.5	1,260.6	E	1,472.6	736.8	1,455.6	1,454.6	13
14	1,379.6	690.3	1,362.6	1,361.6	T	1,343.5	672.3	1,326.5	1,325.5	12
15	1,546.6	773.8	1,529.6	1,528.6	S+80	1,242.5	621.8	1,225.5	1,224.5	11
16	1,617.6	809.3	1,600.6	1,599.6	A	1,075.5	538.3	1,058.5	1,057.5	10
17	1,704.7	852.8	1,687.7	1,686.7	S	1,004.5	502.7	987.4	986.5	9
18	1,833.7	917.4	1,816.7	1,815.7	E	917.4	459.2	900.4	899.4	8
19	1,962.8	981.9	1,945.7	1,944.8	E	788.4	394.7	771.4	770.4	7
20	2,059.8	1,030.4	2,042.8	2,041.8	P	659.3	330.2	642.3	641.3	6
21	2,146.8	1,073.9	2,129.8	2,128.8	S	562.3	281.7	545.3	544.3	5
22	2,245.9	1,123.5	2,228.9	2,227.9	V	475.3	238.1	458.2	457.3	4
23	2,332.9	1,167.0	2,315.9	2,314.9	S	376.2	188.6	359.2	358.2	3
24	2,447.0	1,224.0	2,430.0	2,429.0	N	289.2	145.1	272.1		2
25	2,621.1	1,311.1	2,604.1	2,603.1	R	175.1	88.1	158.1		1

Fig. S8. Fragmentation tables as they appear in the Scaffold program for phosphorylated serines and threonines (S45, S49, S139, T144, S145, and S307) in Atg20. The presence of

phosphorylated serine (S+80) or threonine (T+80) is confirmed by *b* and/or *y* ions that are highlighted in red and blue color.

S342

B	B Ions	B+2H	B-NH3	B-H2O	AA	Y Ions	Y+2H	Y-NH3	Y-H2O	Y
1	114.1	57.5			I	2,016.0	1,008.5	1,999.0	1,998.0	18
2	251.2	126.1			H	1,902.9	952.0	1,885.9	1,884.9	17
3	322.2	161.6			A	1,765.9	883.4	1,748.9	1,747.9	16
4	469.2	235.1			M+16	1,694.8	847.9	1,677.8	1,676.8	15
5	582.3	291.7			L	1,547.8	774.4	1,530.8	1,529.8	14
6	679.4	340.2			P	1,434.7	717.9	1,417.7	1,416.7	13
7	792.4	396.7			I	1,337.7	669.3	1,320.6	1,319.7	12
8	889.5	445.3			P	1,224.6	612.8	1,207.6	1,206.6	11
9	946.5	473.8			G	1,127.5	564.3	1,110.5	1,109.5	10
10	1,033.6	517.3		1,015.5	S	1,070.5	535.8	1,053.5	1,052.5	9
11	1,200.5	600.8		1,182.5	S+80	983.5	492.2	966.5	965.5	8
12	1,287.6	644.3		1,269.6	S	816.5	408.7	799.5	798.5	7
13	1,416.6	708.8	1,399.6	1,398.6	Q+1	729.5	365.2	712.4		6
14	1,529.7	765.4	1,512.7	1,511.7	L	600.4	300.7	583.4		5
15	1,642.8	821.9	1,625.8	1,624.8	L	487.3	244.2	470.3		4
16	1,755.9	878.4	1,738.8	1,737.9	L	374.2	187.6	357.2		3
17	1,869.9	935.5	1,852.9	1,851.9	N	261.2	131.1	244.1		2
18	2,016.0	1,008.5	1,999.0	1,998.0	K	147.1	74.1	130.1		1

S343

B	B Ions	B+2H	B-NH3	B-H2O	AA	Y Ions	Y+2H	Y-NH3	Y-H2O	Y
1	114.1				I	2,015.0	1,008.0	1,998.0	1,997.0	18
2	251.2	126.1			H	1,902.0	951.5	1,884.9	1,883.9	17
3	322.2	161.6			A	1,764.9	883.0	1,747.9	1,746.9	16
4	469.2	235.1			M+16	1,693.9	847.4	1,676.8	1,675.8	15
5	582.3	291.7			L	1,546.8	773.9	1,529.8	1,528.8	14
6	679.4	340.2			P	1,433.7	717.4	1,416.7	1,415.7	13
7	792.4	396.7			I	1,336.7	668.8	1,319.7	1,318.7	12
8	889.5	445.3			P	1,223.6	612.3	1,206.6	1,205.6	11
9	946.5	473.8			G	1,126.6	563.8	1,109.5	1,108.5	10
10	1,033.6	517.3		1,015.5	S	1,069.5	535.3	1,052.5	1,051.5	9
11	1,120.6	560.8		1,102.6	S	982.5	491.8	965.5	964.5	8
12	1,287.6	644.3		1,269.6	S+80	895.5	448.2	878.4	877.5	7
13	1,415.6	708.3	1,398.6	1,397.6	Q	728.5	364.7	711.4		6
14	1,528.7	764.9	1,511.7	1,510.7	L	600.4		583.4		5
15	1,641.8	821.4	1,624.8	1,623.8	L	487.3		470.3		4
16	1,754.9	877.9	1,737.9	1,736.9	L	374.2		357.2		3
17	1,868.9	935.0	1,851.9	1,850.9	N	261.2		244.1		2
18	2,015.0	1,008.0	1,998.0	1,997.0	K	147.1		130.1		1

S361

B	B Ions	B+2H	B-NH3	B-H2O	AA	Y Ions	Y+2H	Y-NH3	Y-H2O	Y
1	168.0	84.5		150.0	S+80	2,991.4	1,496.2	2,974.3	2,973.4	24
2	296.1	148.6	279.1	278.1	K	2,824.4	1,412.7	2,807.3	2,806.4	23
3	383.1	192.1	366.1	365.1	S	2,696.3	1,348.6	2,679.2	2,678.3	22
4	530.2	265.6	513.2	512.2	F	2,609.2	1,305.1	2,592.2	2,591.2	21
5	631.2	316.1	614.2	613.2	T	2,462.2	1,231.6	2,445.1	2,444.2	20
6	745.3	373.1	728.3	727.3	N	2,361.1	1,181.1	2,344.1	2,343.1	19
7	858.4	429.7	841.3	840.4	I	2,247.1	1,124.0	2,230.1	2,229.1	18
8	987.4	494.2	970.4	969.4	E	2,134.0	1,067.5	2,117.0	2,116.0	17
9	1,115.5	558.2	1,098.5	1,097.5	Q	2,005.0	1,003.0	1,987.9	1,986.9	16
10	1,230.5	615.8	1,213.5	1,212.5	D	1,876.9	939.0	1,859.9	1,858.9	15
11	1,393.6	697.3	1,376.5	1,375.6	Y	1,761.9	881.4	1,744.8	1,743.9	14
12	1,521.7	761.3	1,504.6	1,503.7	K	1,598.8	799.9	1,581.8	1,580.8	13
13	1,649.7	825.4	1,632.7	1,631.7	Q	1,470.7	735.9	1,453.7	1,452.7	12
14	1,812.8	906.9	1,795.8	1,794.8	Y	1,342.7	671.8	1,325.6	1,324.6	11
15	1,941.8	971.4	1,924.8	1,923.8	E	1,179.6	590.3	1,162.6	1,161.6	10
16	2,055.9	1,028.4	2,038.8	2,037.9	N	1,050.5	525.8	1,033.5	1,032.5	9
17	2,169.0	1,085.0	2,151.9	2,150.9	L	936.5	468.8	919.5	918.5	8
18	2,282.0	1,141.5	2,265.0	2,264.0	L	823.4	412.2	806.4	805.4	7
19	2,397.1	1,199.0	2,380.0	2,379.1	D	710.3	355.7	693.3	692.3	6
20	2,512.1	1,256.5	2,495.1	2,494.1	N+1	595.3	298.2	578.3		5
21	2,569.1	1,285.1	2,552.1	2,551.1	G	480.3	240.6	463.3		4
22	2,682.2	1,341.6	2,665.2	2,664.2	I	423.3	212.1	406.2		3
23	2,845.3	1,423.1	2,828.2	2,827.2	Y	310.2	155.6	293.1		2
24	2,991.4	1,496.2	2,974.3	2,973.4	K	147.1	74.1	130.1		1

T365

B	B Ions	B+2H	B-NH3	B-H2O	AA	Y Ions	Y+2H	Y-NH3	Y-H2O	Y
1	88.0	44.5		70.0	S	2,991.4	1,496.2	2,974.3	2,973.4	24
2	216.1	108.6	199.1	198.1	K	2,904.3	1,452.7	2,887.3	2,886.3	23
3	303.2	152.1	286.1	285.2	S	2,776.2	1,388.6	2,759.2	2,758.2	22
4	450.2	225.6	433.2	432.2	F	2,689.2	1,345.1	2,672.2	2,671.2	21
5	631.2	316.1	614.2	613.2	T+80	2,542.1	1,271.6	2,525.1	2,524.1	20
6	745.3	373.1	728.3	727.3	N	2,361.1	1,181.1	2,344.1	2,343.1	19
7	858.4	429.7	841.3	840.4	I	2,247.1	1,124.0	2,230.1	2,229.1	18
8	987.4	494.2	970.4	969.4	E	2,134.0	1,067.5	2,117.0	2,116.0	17
9	1,115.5	558.2	1,098.5	1,097.5	Q	2,005.0	1,003.0	1,987.9	1,986.9	16
10	1,230.5	615.8	1,213.5	1,212.5	D	1,876.9	939.0	1,859.9	1,858.9	15
11	1,393.6	697.3	1,376.5	1,375.6	Y	1,761.9	881.4	1,744.8	1,743.9	14
12	1,521.7	761.3	1,504.6	1,503.7	K	1,598.8	799.9	1,581.8	1,580.8	13
13	1,649.7	825.4	1,632.7	1,631.7	Q	1,470.7	735.9	1,453.7	1,452.7	12
14	1,812.8	906.9	1,795.8	1,794.8	Y	1,342.7	671.8	1,325.6	1,324.6	11
15	1,941.8	971.4	1,924.8	1,923.8	E	1,179.6	590.3	1,162.6	1,161.6	10
16	2,056.9	1,028.9	2,039.8	2,038.8	N+1	1,050.5	525.8	1,033.5	1,032.5	9
17	2,169.9	1,085.5	2,152.9	2,151.9	L	935.5	468.3	918.5	917.5	8
18	2,283.0	1,142.0	2,266.0	2,265.0	L	822.4	411.7	805.4	804.4	7
19	2,398.0	1,199.5	2,381.0	2,380.0	D	709.4	355.2	692.3	691.3	6
20	2,512.1	1,256.5	2,495.1	2,494.1	N	594.3	297.7	577.3		5
21	2,569.1	1,285.1	2,552.1	2,551.1	G	480.3	240.6	463.3		4
22	2,682.2	1,341.6	2,665.2	2,664.2	I	423.3	212.1	406.2		3
23	2,845.3	1,423.1	2,828.2	2,827.2	Y	310.2	155.6	293.1		2
24	2,991.4	1,496.2	2,974.3	2,973.4	K	147.1	74.1	130.1		1

S363

B	B Ions	B+2H	B-NH3	B-H2O	AA	Y Ions	Y+2H	Y-NH3	Y-H2O	Y
1	88.0			70.0	S	1,539.7	770.3	1,522.6	1,521.7	12
2	216.1	108.6	199.1	198.1	K	1,452.6	726.8	1,435.6	1,434.6	11
3	383.1	192.1	366.1	365.1	S+80	1,324.5	662.8	1,307.5	1,306.5	10
4	530.2	265.6	513.2	512.2	F	1,157.5	579.3	1,140.5	1,139.5	9
5	631.2	316.1	614.2	613.2	T	1,010.5	505.7	993.5	992.5	8
6	745.3	373.1	728.3	727.3	N	909.4	455.2	892.4	891.4	7
7	858.4	429.7	841.3	840.4	I	795.4	398.2	778.4	777.4	6
8	987.4	494.2	970.4	969.4	E	682.3		665.3	664.3	5
9	1,115.5	558.2	1,098.5	1,097.5	Q	553.3		536.2	535.3	4
10	1,230.5	615.8	1,213.5	1,212.5	D	425.2		408.2	407.2	3
11	1,393.6	697.3	1,376.5	1,375.6	Y	310.2		293.1		2
12	1,539.7	770.3	1,522.6	1,521.7	K	147.1		130.1		1

T517

B	B Ions	B+2H	B-NH3	B-H2O	AA	Y Ions	Y+2H	Y-NH3	Y-H2O	Y
1	88.0	44.5		70.0	S	1,975.9	988.5	1,958.9	1,957.9	18
2	225.1	113.1		207.1	H	1,888.9	944.9	1,871.8	1,870.9	17
3	406.1	203.6		388.1	T+80	1,751.8	876.4	1,734.8	1,733.8	16
4	519.2	260.1		501.2	I	1,570.8	785.9	1,553.8	1,552.8	15
5	633.2	317.1	616.2	615.2	N	1,457.7	729.4	1,440.7	1,439.7	14
6	746.3	373.7	729.3	728.3	L	1,343.7	672.3	1,326.6	1,325.7	13
7	875.4	438.2	858.3	857.4	E	1,230.6	615.8	1,213.6	1,212.6	12
8	1,031.5	516.2	1,014.4	1,013.5	R	1,101.5	551.3	1,084.5	1,083.5	11
9	1,128.5	564.8	1,111.5	1,110.5	P	945.4	473.2	928.4	927.4	10
10	1,242.6	621.8	1,225.5	1,224.6	N	848.4	424.7	831.4	830.4	9
11	1,356.6	678.8	1,339.6	1,338.6	N	734.3	367.7	717.3	716.3	8
12	1,470.6	735.8	1,453.6	1,452.6	N	620.3	310.7	603.3	602.3	7
13	1,571.7	786.4	1,554.7	1,553.7	T	506.3	253.6	489.2	488.2	6
14	1,628.7	814.9	1,611.7	1,610.7	G	405.2	203.1	388.2	387.2	5
15	1,715.7	858.4	1,698.7	1,697.7	S	348.2	174.6	331.2	330.2	4
16	1,772.8	886.9	1,755.7	1,754.8	G	261.2	131.1	244.1		3
17	1,829.8	915.4	1,812.8	1,811.8	G	204.1	102.6	187.1		2
18	1,975.9	988.5	1,958.9	1,957.9	K	147.1	74.1	130.1		1

Fig. S9. Fragmentation tables as they appear in the Scaffold program for phosphorylated serines and threonines (S342, S343, S361, S363, T365, and T517) in Atg20. The presence of phosphorylated serine (S+80) or threonine (T+80) is confirmed by *b* and/or *y* ions that are

highlighted in red and blue color. Phosphorylation on Ser361 was confirmed by peptide mass only.

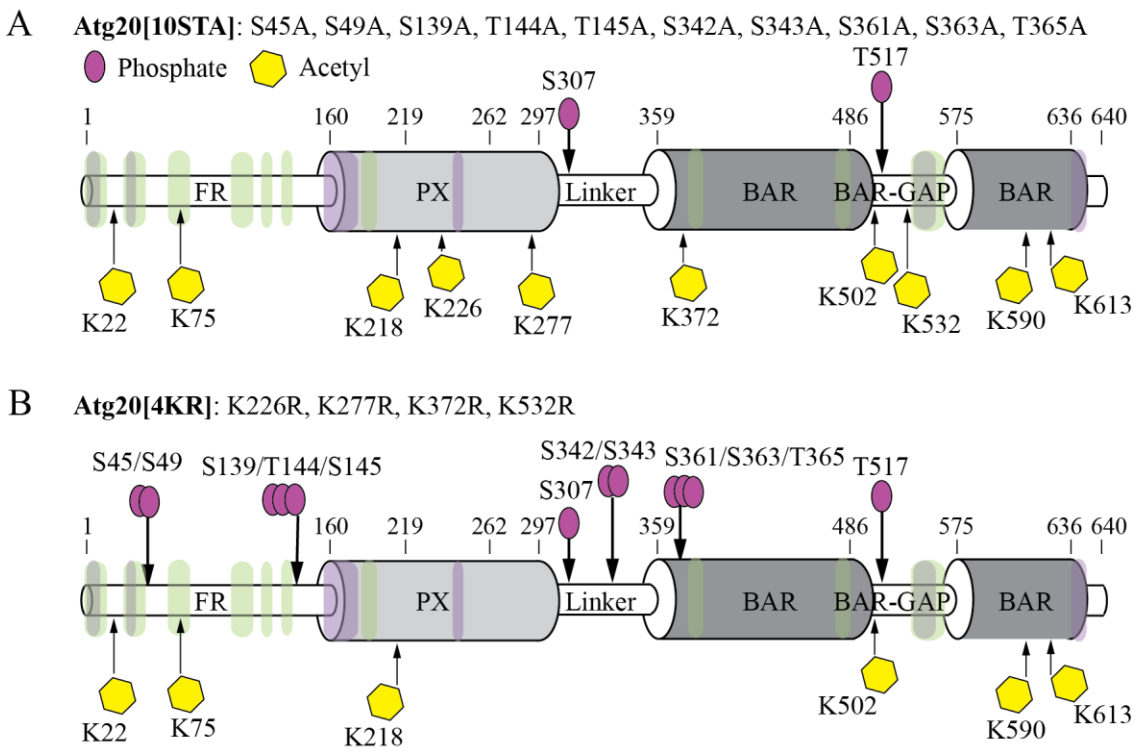

Fig. S10. Schematic representations of Atg20[10STA] and Atg20[4KR]. The representations depict which post-translational modifications were removed and which remained in the mutated Atg20[10STA] (*A*) and Atg20[4KR] (*B*) proteins.

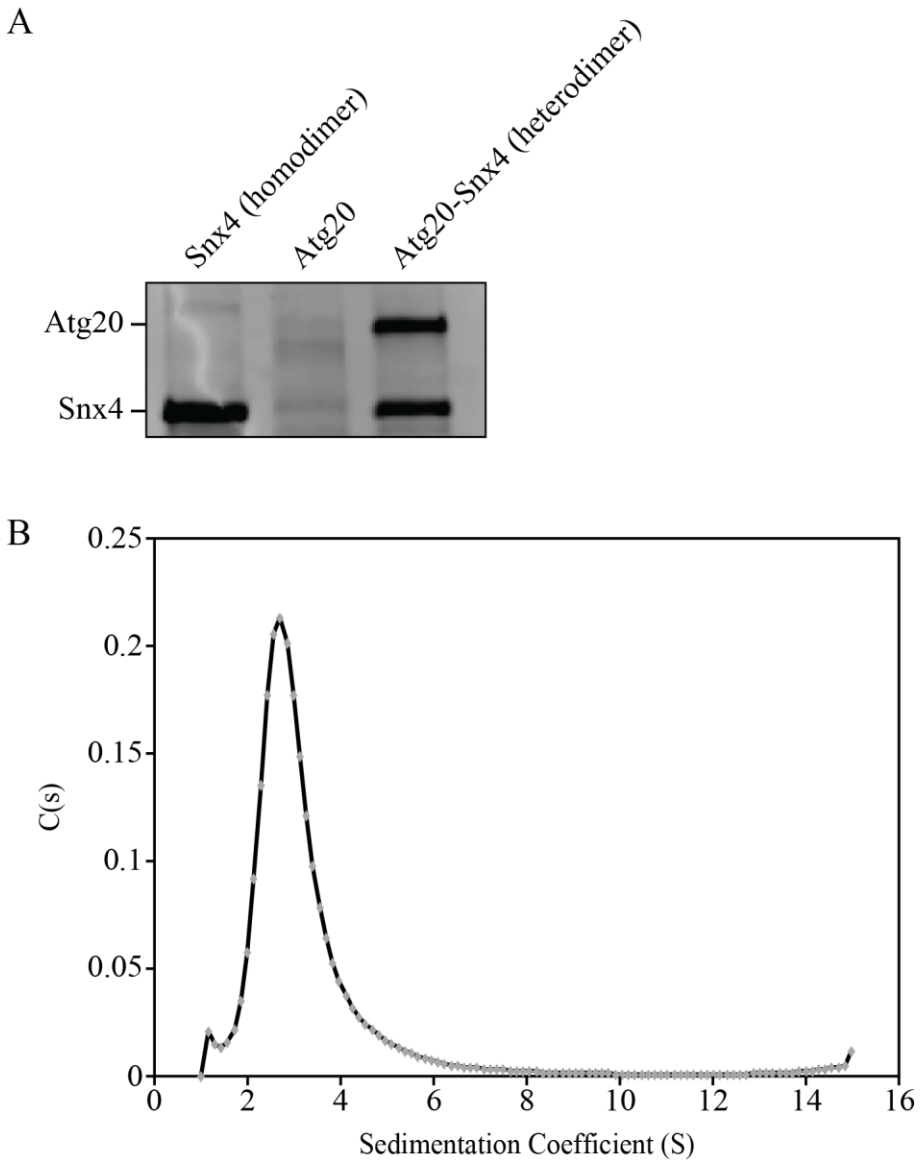

Fig. S11. Structural analysis of the sorting nexins Atg20 and Snx4. (*A*) SDS-PAGE gel showing the capture of full-length Atg20 only as a heterodimer with full-length Snx4. The full-length Snx4 can also form homodimers, but no monomeric or dimeric Atg20 can be captured. (*B*) The AUC data for the $Snx4_{421-423}$ homodimer. The molecular mass determined by dynamic light scattering for this homodimer is 93.3 kDa, which is very similar to the expected molecular mass of 93.7 kDa.

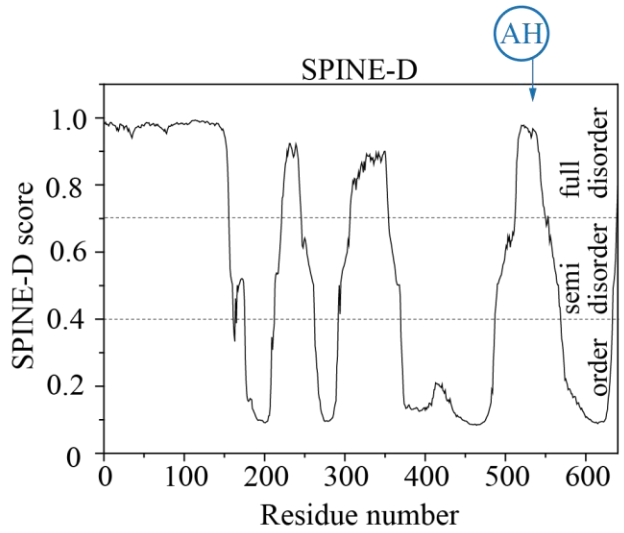

MFDp2

GREEN letters represent residues predicted as ordered
RED letters correspond to predicted disordered residues

SEQ Predicted disorder content: 35.47 %; # of disorder segments: 2

```
        10        20        30        40        50        60        70        80
MSDLNDVQEN AKLNSETRNT GKAEPPHGTT EYVAEAEISK NGVGSPKKSP KKGKVGKGDN NKVETELVHT ALLEKDNPFM
        90       100       110       120       130       140       150       160
EEGPTGFTKS ALLEIPGMRS HNLKNPNEDY EDDSEGLLPL NQESNAETCR TSLSGSINSM NGETSASEEP SVSNRKKSAR
       170       180       190       200       210       220       230       240
IHILEAKRVS EGQGRAYIAY VIQFENSTVQ RRYSDFESLR SILIRLFPMT LIPPIPEKQS IKNYGKSITG SSSKYLLPSE
       250       260       270       280       290       300       310       320
GSGSVDLSLS VIHASVNNSD EKLIRHRIRM LTEFLNKLLT NEEITKTSII TDFLDPNNHN WHEFVNSSST FSSLPKSILQ
       330       340       350       360       370       380       390       400
CNPLDPTNTT RIHAMLPIPG SSSQLLLNKE SNDKKMDKER SKSFTNIEQD YKQYENLLDN GIYKYNRRTT KTYHDLKSDY
       410       420       430       440       450       460       470       480
NEIGEVFAQF AHEQAQVGEL AEQLSYLSNA FSGSSISLEK LVGRLYYNIN EPLNESVHMA TSARELIKYR KLKYLQNEMI
       490       500       510       520       530       540       550       560
KKSLNSKRAQ LEKLEAQNNE YKDVDKIIDN EMSKSHTINL ERPNNNTGSG GKSYGGKLFN GFNKLASMVK DSVKYQETDP
       570       580       590       600       610       620       630       640
HTASINLKKE IEQLSESLEV TENDLEVISK VIKNDQLPKF SKEREVDLSE ILKHYSRYMR NYARQNLEIW KEVKRHQDFA
```

AH

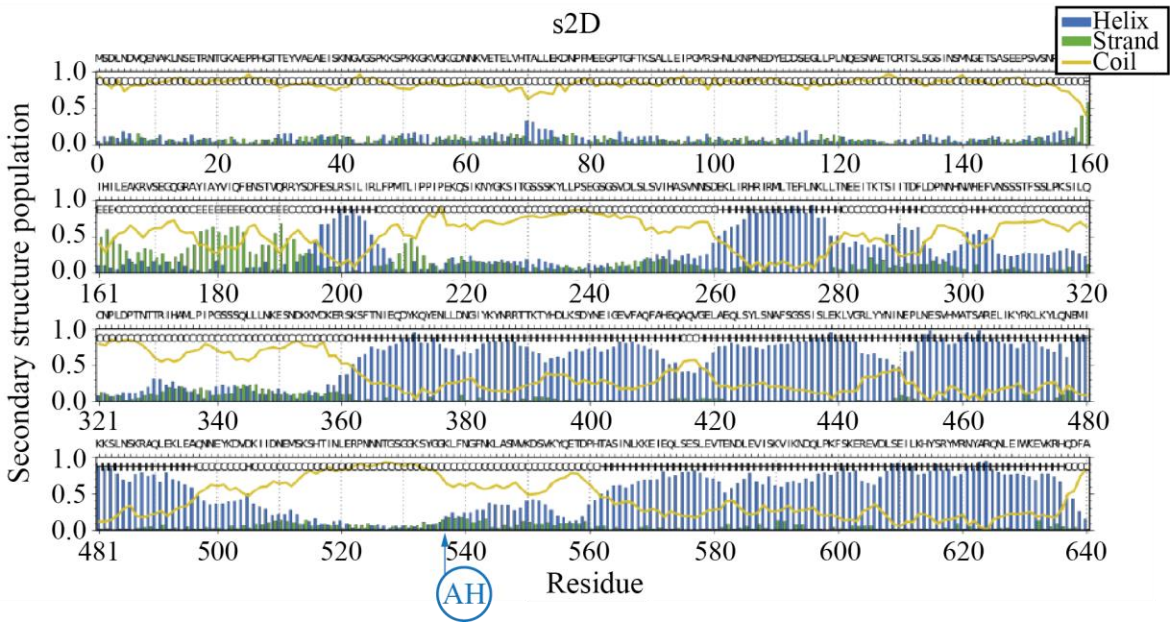

Fig. S12. Analysis of the amino acid sequence of Atg20 by predictors (SPINE-D, MFDp2, and s2D; (2-4)) for intrinsically disordered protein regions. The position of the putative amphipathic helix (AH) in Atg20 is indicated by a blue arrow.

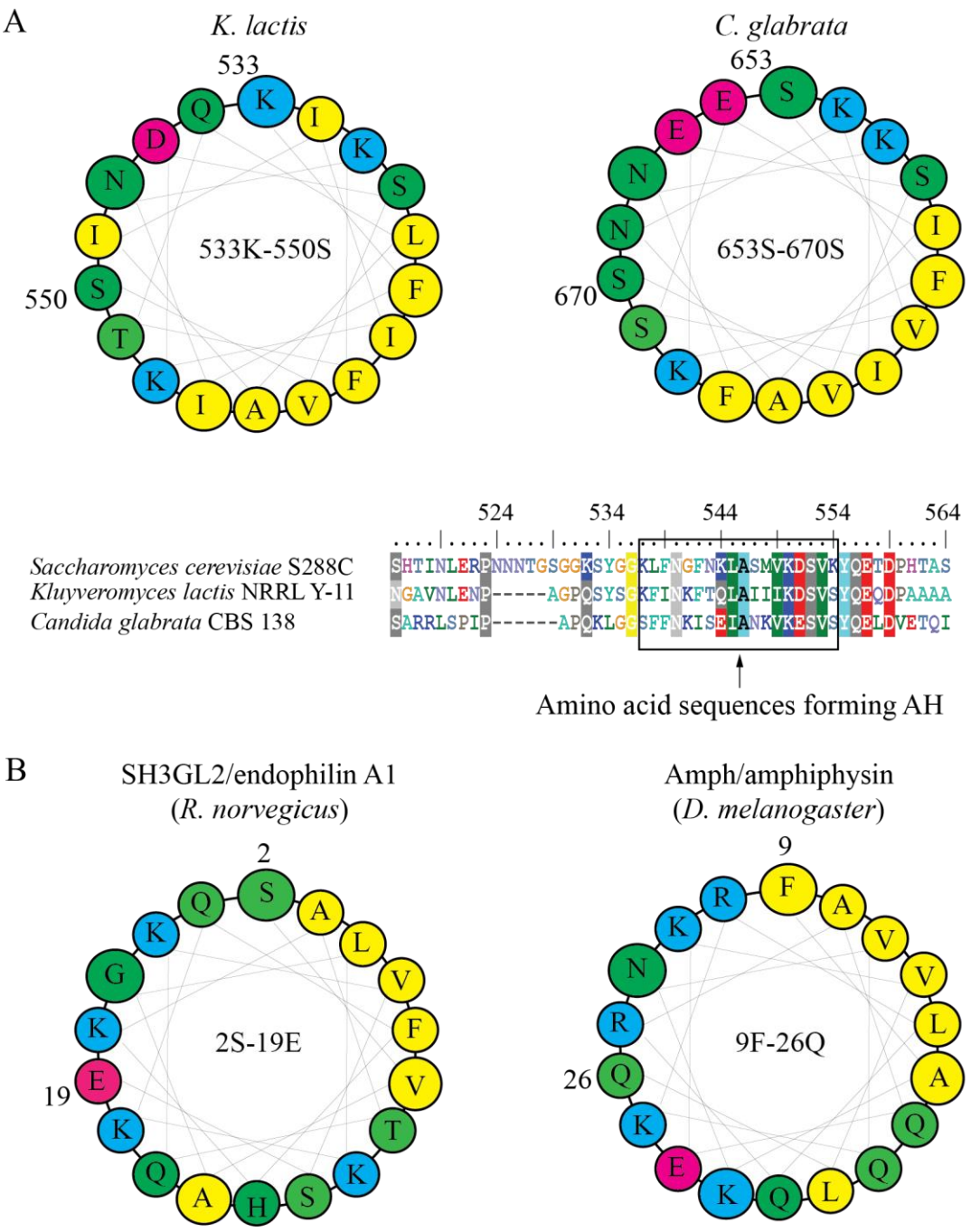

Fig. S13. Comparison of predicted amphipathic helices in fungal Atg20 homologs and BAR domain-containing proteins. (*A*) AH in Atg20 of *K. lactis* and *C. glabrata* formed by amino acids sequences homologous to the amino acid sequence forming AH in Atg20 of *S. cerevisiae*. (*B*) AH in SH3GL2/endophilin A1 and Amph/mphiphysin (5) are shown for comparison with those in (*A*).

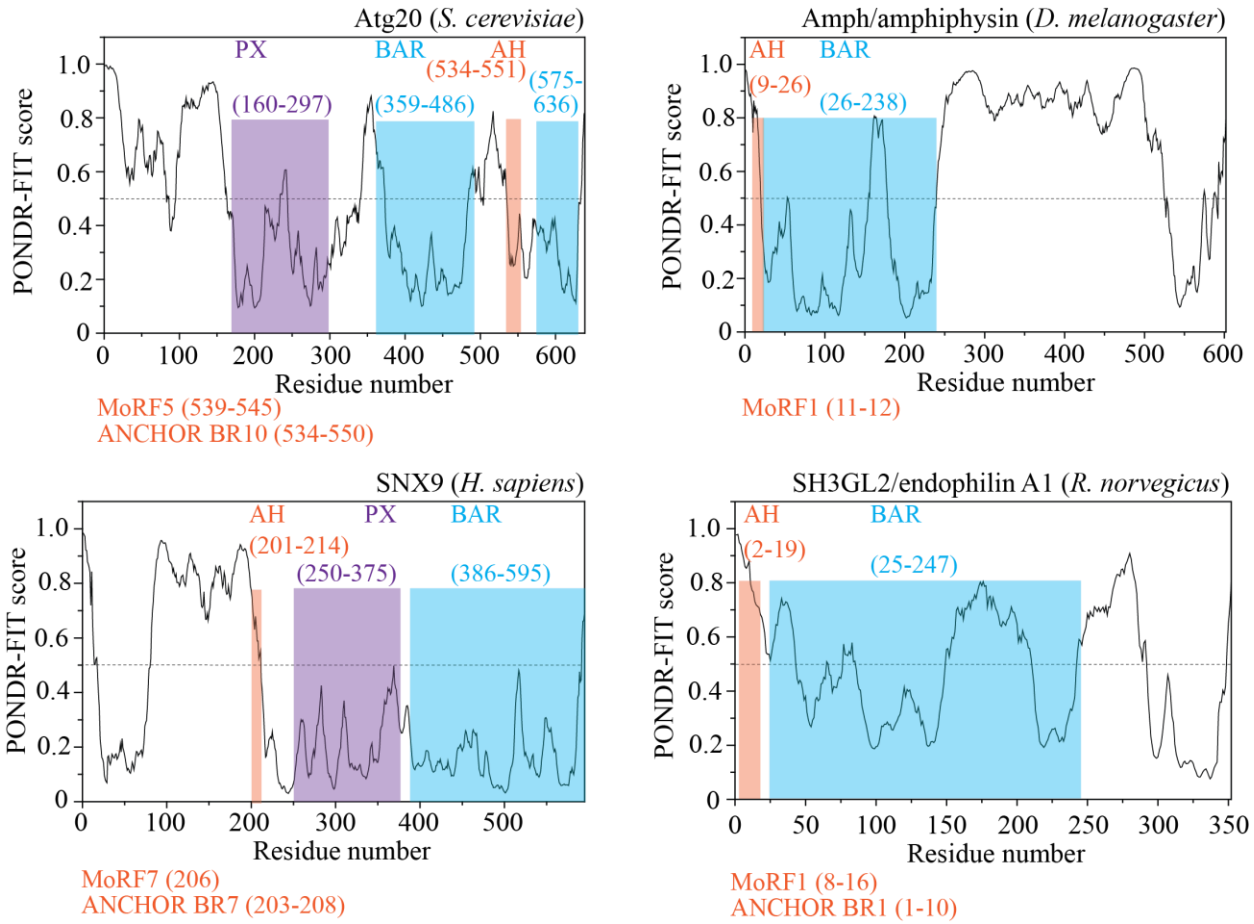

Fig. S14. Comparative bioinformatics analysis of the amino acids sequences of the BAR proteins that encompass a membrane-inducible AH. The consensus sequences for the BAR and PX domains, as determined by protein-protein BLAST, are indicated in blue and purple, respectively. The position of a particular AH within an IDPR determined by PONDR-FIT is shown in red. The results of the algorithms MoRFPred and ANCHOR (if any), which determine the position of a foldable element (termed molecular recognition feature or ANCHOR disordered binding domain) within an IDPR, is indicated in red for each BAR protein under the corresponding diagram.

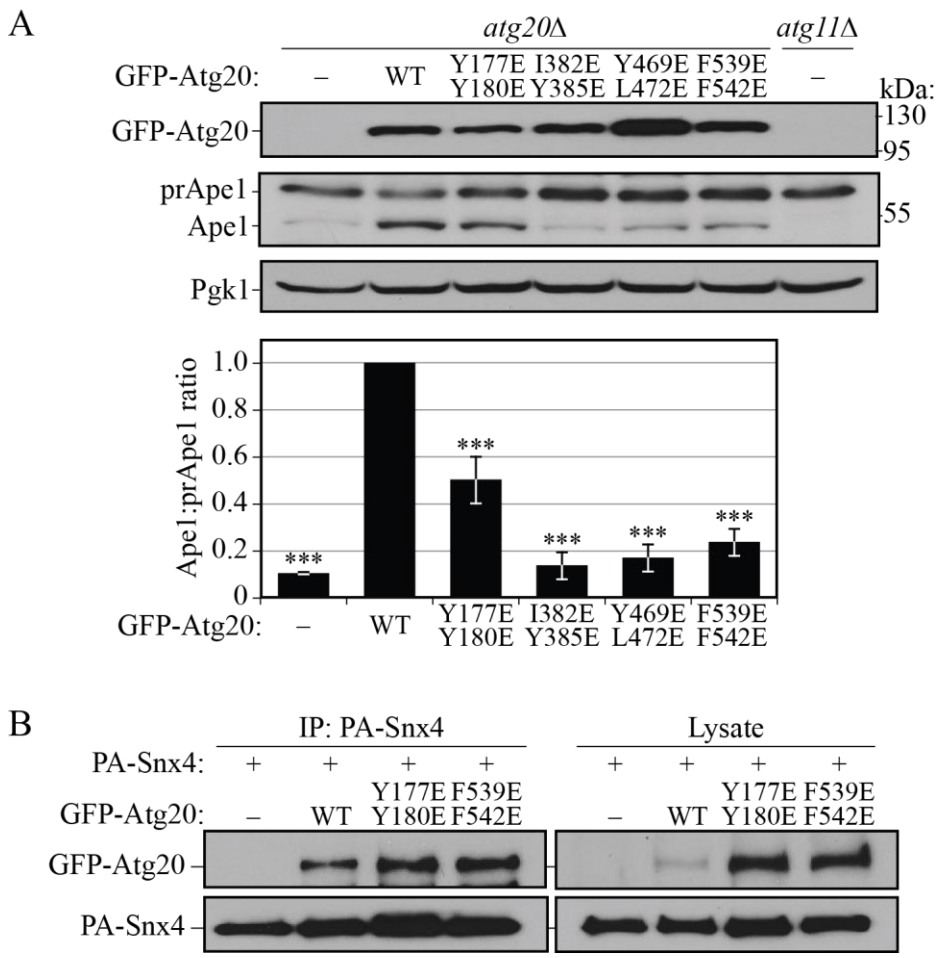

Fig. S15. Analysis of mutations in the PX, BAR, and BAR-GAP domains of Atg20. (*A*) The structural mutants of Atg20 are defective in the Cvt pathway. The *atg20*Δ strain (D3Y009) was transformed with the plasmid pCuGFP(426), pCuGFP-Atg20(426), pCuGFP-Atg20[Y177E Y180/E](426), pCuGFP-Atg20[I382E Y385E](426), pCuGFP-Atg20[Y469E L472E](426) or pCuGFP-Atg20[F539E F542E](426). The *atg11*Δ (SEY6210) strain was used as a negative control. GFP, Ape1 and Pgk1 (loading control) were detected from the cell lysate by immunoblotting. Columns are averages and error bars represent standard deviation from 3 independent experiments. Statistical significance was tested by unpaired two-tailed Student's t-test. The p values less than 0.005 were considered to be significant (***). (*B*) PA-Snx4 co-precipitates all variants of GFP-Atg20. The plasmids pCuGFP(426), pCuGFP-Atg20(426), pCuGFP-Atg20[Y177E Y180/E](426), or pCuGFP-Atg20[F539E F542E](426) were transformed into MKO (YCY123) cells and co-expressed under the *CUP1* promotor with the pCuPA-Snx4(424) plasmid. Cells were cultured in SMD, and cell lysates were prepared and incubated

with IgG-Sepharose for affinity purification. The proteins were separated by SDS-PAGE and detected with monoclonal antibody that recognizes GFP or PA. The F539E F542E mutation in MoRF5/BR10 does not weaken the interaction between Atg20 and Snx4.

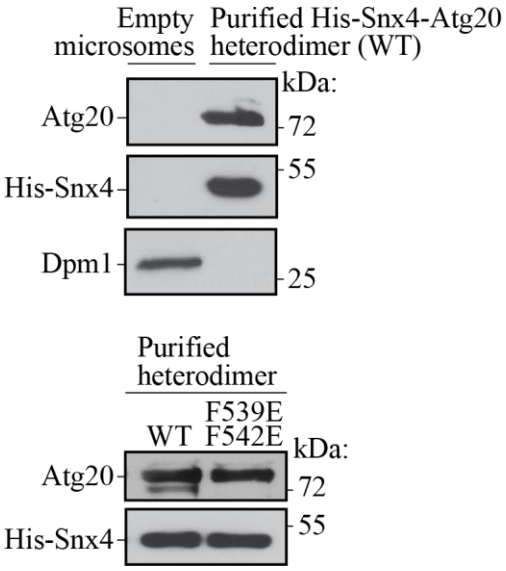

Fig. S16. Analysis of the microsomes and protein input for the *in vitro* membrane-binding assay. Upper panel, western blots showing the presence of Atg20 and His-Snx4 in the recombinant purified heterodimer and the presence of the endoplasmic reticulum marker protein Dpm1 in microsomes isolated from *snx4*Δ *atg20*Δ (SEY6210) cells; lower panel, western blots showing an equal input of purified heterodimers (wild-type or mutant) that were used in the reconstitution experiment.

Table S1. *S. cerevisiae* strains used in this study.

Name	Genotype	Reference
CWY230	*SEY6210 vac8Δ::KAN*	(6)
D3Y009	*SEY6210 atg20Δ::HIS*	This study
HPY017	*SEY6210 atg24Δ::HIS, atg20Δ::LEU2*	This study
HPY063	*WLY176 atg20Δ::LEU2*	This study
HPY079	*CWY230 atg20Δ::HIS3*	This study
HPY081	W303-1B *vac8Δ::URA3*	This study
HPY082	W303-1B *vac8Δ::URA3 atg20Δ::KAN*	This study
SEY6210	*MATα leu2-3,112 ura3-52 his3-Δ200 trp1-Δ901 lys2-801 suc2-Δ9 GAL*	(7)
W303-1B	*MATα leu2-3,112 ura3-1 his3-11,15 trp1-1, ade2-1 can1-100*	(8)
WLY176	*SEY6210 pho13Δ pho8Δ60*	This study
YAB87	ZFY202 *atg20Δ::KAN*	This study
YCY123	*SEY6210 atg1Δ, 2Δ, 3Δ, 4Δ, 5Δ, 6Δ, 7Δ, 8Δ, 9Δ, 10Δ, 11Δ, 12Δ, 13Δ, 14Δ, 16Δ, 17Δ, 18Δ, 19Δ, 20Δ, 21Δ, 23Δ, 24Δ, 27Δ, 29Δ,*	(9)
YTS147	*SEY6210 atg11Δ::LEU2*	This study
ZFY202	W303-1B *pho13Δ pho8Δ60*	This study

SI References

1. Hall TA (1999) BioEdit: a user-friendly biological sequence alignment editor and analysis program for Windows 95/98/NT. *Nucleic Acids Symposium Series* 41:95-98.
2. Zhang T, *et al.* (2012) SPINE-D: accurate prediction of short and long disordered regions by a single neural-network based method. *J Biomol Struct Dyn* 29(4):799-813.
3. Mizianti MJ, Peng Z, & Kurgan L (2013) MFDp2 Accurate predictor of disorder in proteins by fusion of disorder probabilities, content and profiles. *Intrinsically Disordered Proteins* 1(1):e24428.
4. Sormanni P, Camilloni C, Fariselli P, & Vendruscolo M (2015) The s2D Method: Simultaneous Sequence-Based Prediction of the Statistical Populations of Ordered and Disordered Regions in Proteins. *J Mol Biol* 427(4):982-996.
5. Bhatia VK, *et al.* (2009) Amphipathic motifs in BAR domains are essential for membrane curvature sensing. *EMBO J* 28(21):3303-3314.
6. Umekawa M & Klionsky DJ (2012) Ksp1 kinase regulates autophagy via the target of rapamycin complex 1 (TORC1) pathway. *J Biol Chem* 287(20):16300-16310.
7. Robinson JS, Klionsky DJ, Banta LM, & Emr SD (1988) Protein sorting in Saccharomyces cerevisiae: isolation of mutants defective in the delivery and processing of multiple vacuolar hydrolases. *Mol Cell Biol* 8(11):4936-4948.
8. Thomas BJ & Rothstein R (1989) Elevated recombination rates in transcriptionally active DNA. *Cell* 56(4):619-630.
9. Cao Y, Cheong H, Song H, & Klionsky DJ (2008) In vivo reconstitution of autophagy in Saccharomyces cerevisiae. *J Cell Biol* 182(4):703-713.